

Radial overlap correction to superallowed $0^+ \rightarrow 0^+$ β decay reexamined

L. Xayavong and N. A. Smirnova

CENBG (CNRS/IN2P3 - Université de Bordeaux), Chemin du Solarium, 33175 Gradignan, France



(Received 31 July 2017; revised manuscript received 31 October 2017; published 21 February 2018)

Within the nuclear shell model, we investigate the correction δ_{RO} to the Fermi matrix element due to a mismatch between proton and neutron single-particle radial wave functions. Eight superallowed $0^+ \rightarrow 0^+$ β decays in the *sd* shell, comprising ^{22}Mg , ^{26m}Al , ^{26}Si , ^{30}S , ^{34}Cl , ^{34}Ar , ^{38m}K , and ^{38}Ca , are reexamined. The radial wave functions are obtained from a spherical Woods-Saxon potential whose parametrizations are optimized in a consistent adjustment of the depth and the length parameters to relevant experimental observables, such as nucleon separation energies and charge radii, respectively. The chosen fit strategy eliminates the strong dependence of the radial mismatch correction to a specific parametrization, except for calculations with an additional surface-peaked term. As an improvement, our model proposes a new way to calculate the charge radii, based on a parentage expansion which accounts for correlations beyond the extreme independent-particle model. Apart from the calculations with a surface-peak term and the cases where we used a different model space, the new sets of δ_{RO} are in general agreement with the earlier result of Towner and Hardy [Phys. Rev. C **66**, 035501 (2002)]. Small differences of the corrected average $\overline{\mathcal{F}t}$ value are observed.

DOI: [10.1103/PhysRevC.97.024324](https://doi.org/10.1103/PhysRevC.97.024324)

I. INTRODUCTION

The superallowed nuclear β decay between 0^+ , $T = 1$ isobaric analog states has long been known as a sensitive tool to probe the fundamental symmetries underlying the standard model of electroweak interaction. According to the conserved vector current (CVC) hypothesis, the corrected $\mathcal{F}t$ value or equivalently the vector coupling constant G_V must be nucleus independent. If CVC holds, those constants can be used to extract $|V_{ud}|$, the absolute value of the up-down element of the Cabibbo-Kobayashi-Maskawa (CKM) quark-mixing matrix. This value, combined with the complementary experimental data on $|V_{us}|$ and $|V_{ub}|$, the other top-row matrix elements, provides the most accurate test of the unitarity of the CKM matrix (see Ref. [1] for details and the present status).

Nowadays, 14 transitions ranging from ^{10}C to ^{74}Rb are known experimentally with a precision of 0.1% or better, therefore we must consider all kinds of side effects of this order of magnitude before deducing the $\mathcal{F}t$ value. All previous investigations (Ref. [1] and references therein) indicate that the current uncertainty on $|V_{ud}|$ is dominated by a set of theoretical corrections aimed to account for the radiative effects and the isospin-symmetry breaking in nuclear states. The latter is strongly structure dependent and has the greatest effect on reducing the scatter in the $\mathcal{F}t$ values.

Since superallowed $0^+ \rightarrow 0^+$ β decay is governed uniquely by the vector part of the electroweak current, the corrected $\mathcal{F}t$ value can be deduced from the expression [2]

$$\begin{aligned} \mathcal{F}t &= ft(1 + \delta'_R)(1 + \delta_{NS} - \delta_C) \\ &= \frac{K}{2G_V^2(1 + \Delta_R^V)} = \text{const}, \end{aligned} \quad (1)$$

where K is a combination of fundamental constants $K = 2\pi^3 \hbar \ln 2 (\hbar c)^6 / (m_e c^2)^5 = (8120.2716 \pm 0.012) \times 10^{-10} \text{ GeV}^{-4} \text{ s}$, and ft is the product of the statistical rate function (f) [3] and the partial half-life (t). The radiative corrections are separated into three parts [1]: $\Delta_R^V = 2.361(38)\%$ is nucleus independent, δ'_R depends on the atomic number of daughter nucleus, and δ_{NS} is nuclear-structure dependent. The correction due to the isospin-symmetry breaking, δ_C , is defined as the deviation of the realistic Fermi matrix element squared from its isospin-symmetry value,

$$|M_F|^2 = |M_F^0|^2(1 - \delta_C), \quad (2)$$

with $|M_F^0| = \sqrt{T(T+1) - T_{zi}T_{zf}} = \sqrt{2}$ for the $T = 1$ case.

Over the past 40 years, various theoretical approaches have been applied to get δ_C . Figure 1 shows the results of calculations performed within different microscopic models for a large ensemble of emitters. Towner and Hardy [2,4,5] use the shell model with radial wave functions derived from a Woods-Saxon (WS) potential. Some time ago, Ormand and Brown [6,7] performed shell-model calculations using Skyrme Hartree-Fock (HF) radial wave functions (see also our recent study in Ref. [8]). The obtained corrections are systematically smaller than those obtained from WS wave functions. Spin and isospin projected HF calculations based on two different parametrizations of the Skyrme energy density functional have been realized by Satula *et al.* [9]. Except for a few cases, their values for light and medium-mass nuclei are on average of the same order of magnitude as those found within the shell-model approach. For $A = 34$ emitters, Satula *et al.* obtain quite large corrections compared to the shell model. However, at the same time they assign large theoretical uncertainties on those values, so the agreement roughly holds. Another approach in which random-phase approximation (RPA) correlations have been

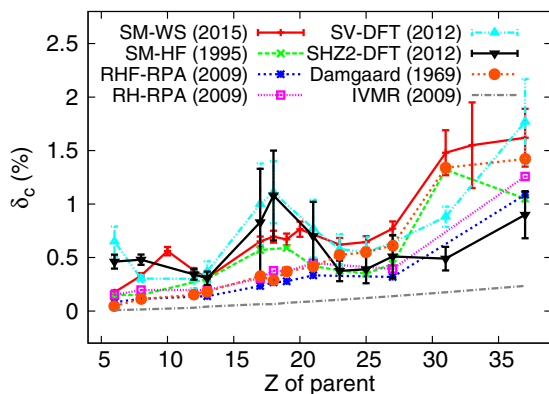


FIG. 1. Isospin-symmetry breaking correction δ_C obtained from different models: shell model with WS radial wave functions (SM-WS) [2,4,5], shell model with HF wave functions (SM-HF) [6,7], $J(T)$ -projected HF theory with two different Skyrme functionals (SV-DFT and SHZ2-DFT) [9], relativistic RPA (RHF-RPA and RH-RPA) [10], isovector monopole resonance theory (IVMR) [11], and the Damgaard model [12].

added to a relativistic Hartree or Hartree-Fock (HF) calculation was used by Liang *et al.* [10]. In addition, Auerbach [11] uses a model where the main isospin-symmetry-breaking effects are attributed to the isovector monopole resonance. The last two results are again systematically lower than the shell-model or $J(T)$ -projected HF values. For completeness, we show also an earlier estimation of the correction using perturbation theory on the basis of individual harmonic-oscillator wave functions by Damgaard [12]. It is clear that all these calculations have a significant spread in the obtained values of δ_C , thus raising the question of credibility of the results.

The values for δ_C tabulated by Towner and Hardy in Ref. [1] excellently support both the CVC hypothesis over the full range of Z values and the top-row unitarity of the CKM matrix. However, this agreement is not sufficient to reject the other calculations, since these aspects of the standard model have to be confirmed experimentally. The validity of CVC does not constrain the absolute $\mathcal{F}t$ value. The disagreement between model predictions and the importance of the issue motivated us to reexamine this correction in a consistent approach based on the nuclear shell model.

Within the shell model, the eigenproblem is solved by construction and diagonalization of the Hamiltonian matrix using a Slater determinant spherical harmonic-oscillator basis. The eigenstates are thus given in terms of linear combinations of many-body basis states. In order to describe isospin-symmetry breaking effects, the many-body Hamiltonian should contain Coulomb and charge-dependent terms of nuclear origin. If the eigenproblem is solved in a sufficiently large A -body basis of many harmonic-oscillator shells, the eigenvectors can be used to compute a realistic Fermi matrix elements, as, for example, has been done for ^{10}C in the no-core shell model with $3N$ forces included [13]. However, for heavier nuclei, calculations are feasible only in restricted model spaces, containing one or two harmonic-oscillator shells beyond a closed-shell core. Effective isospin-nonconserving interaction introduces the isospin-symmetry breaking in the mixing of

various harmonic-oscillator configurations within the model space. In addition, calculation of transition matrix elements involves radial integrals which should be computed using realistic spherically symmetric proton and neutron wave functions, obtained from a finite-range potential with a Coulomb term. The protons in a parent nucleus are less bound than the neutrons in a daughter nucleus because of the Coulomb repulsion. Since the model space is restricted to a single oscillator shell, in practice the only way to deal with the problem is to replace the harmonic-oscillator radial wave functions by single-particle wave functions obtained from a realistic spherically symmetric mean-field potential. This accounts for the isospin-symmetry breaking effects beyond the valence space. Thus, there are two sources of the deviation of the Fermi matrix element from its model-independent value: one is from the effective charge-dependent Hamiltonian and the other is from the radial mismatch of proton and neutron single-particle wave functions. It will be shown below that, within the first-order perturbation theory, the correction δ_C can be expressed as a sum of two terms corresponding to the two sources of isospin-symmetry breaking mentioned above.

The present study focuses on the radial mismatch between proton and neutron single-particle wave functions, which represents the main contribution to the nuclear structure correction to the Fermi matrix element. Currently, two types of a mean-field potential are considered in this respect. The first one is the phenomenological WS potential including a central, a spin-orbit, and an electrostatic repulsion term. A series of calculations using this potential has been carried out by Towner and Hardy [2,4]. These authors adjusted case-by-case the depth of the volume term or added an additional surface-peak term to reproduce experimental proton and neutron separation energies. In addition, they adjusted the length parameter of the central term to fix the charge radii of the parent nuclei. The second type of a mean-field potential is that obtained from self-consistent HF calculations using a zero-range Skyrme force, as was first proposed by Ormand and Brown in 1985 [14] and refined in the subsequent papers [6,7].

The results obtained from both types of mean-field potential are equivalently in good agreement with the CVC hypothesis; however, the δ_C values from Skyrme-HF calculations are consistently smaller than those obtained from the WS calculations. This discrepancy was thought to be due to the insufficiency of the Slater approximation for treating the Coulomb exchange term. Towner and Hardy highlighted that the asymptotic limit of the Coulomb potential in the Slater approximation is overestimated by one unit of Z . To retain this property, they proposed a modified HF protocol [5], namely they performed a single calculation for the nucleus with $(A - 1)$ nucleons and $(Z - 1)$ protons and then used the proton and the neutron eigenfunctions from the same calculation to compute the radial overlap integrals. Their result leads to a significant increase of the corresponding correction to the Fermi matrix element and provides a better agreement with the values obtained with WS radial wave functions. However, we warn that such a method is rooted in Koopman's theorem, which is not fully respected by the HF calculations, in particular with a density-dependent effective interaction.

In the present paper, we propose a comprehensive and detailed study of the radial-overlap correction to superallowed $0^+ \rightarrow 0^+$ β -decay matrix elements using the nuclear shell model with WS single-particle wave functions. A special emphasis is given on the choice of the WS potential parametrization and optimization procedure. We limit ourselves to the sd -shell nuclei, for which very precise shell-model wave functions are available. Once the method is established, we plan to extend this study to heavier emitters, using large-scale shell-model diagonalization and modern effective interactions.

The article is organized as follows. The general formalism is given in Sec. II. Section III discusses the selection of a WS potential parametrization. In Sec. IV, we carry out a simplified calculation of radial-overlap correction to the Fermi matrix element in the closure approximation. The sensitivity to the parameters and the adjustment procedure is investigated. In Sec. V, we present our final results, obtained from a full parentage expansion for both the radial-overlap correction and charge radii of the parent nuclei. The charge radii are computed using two different methods with respect to the treatment of closed-shell orbits. In Sec. VI, we use the obtained results to get the weighted averages of the $\mathcal{F}t$ values for six sd -shell emitters for which the measured ft values have attained the level of precision currently required for the tests of the standard model. In Sec. VII, the sets of radial-overlap corrections are tested against the experimental data, under the assumption that the CVC hypothesis is valid. Comparisons with the previously published values are made. The summary and concluding remarks are given in Sec. VIII.

II. GENERAL FORMALISM

Within the nuclear shell model, the Fermi matrix element for the superallowed β^+ decay can be expressed [2,14] as

$$M_F = \langle \psi_f | t_+ | \psi_i \rangle, \quad (3)$$

where t_+ is the isospin raising operator and $|i\rangle$ and $|f\rangle$ denote the initial and the final nuclear states, respectively. In the second quantization, and using the proton-neutron formalism, we can expand this matrix element in terms of one-body transition densities and single-particle matrix elements as

$$M_F = \sum_{\alpha} \langle f | a_{\alpha_n}^{\dagger} a_{\alpha_p} | i \rangle \langle \alpha_n | t_+ | \alpha_p \rangle. \quad (4)$$

In this equation the operator a_{α} destroys a nucleon in quantum state α whereas the operator a_{α}^{\dagger} creates a nucleon in that state, with α standing for the whole set of spherical quantum numbers, $\alpha = (n_{\alpha}, l_{\alpha}, j_{\alpha}, m_{\alpha})$; the labels n and p refer to neutron and proton quantum states, respectively. Following the previous work within the shell model of Towner and Hardy [2,4] and that of Ormand and Brown [6,14], we suppose that the single-particle matrix element is given by an overlap of the proton [$R_{\alpha_p}(r)$] and neutron [$R_{\alpha_n}(r)$] radial wave functions:

$$\langle \alpha_n | t_+ | \alpha_p \rangle = \int_0^{\infty} R_{\alpha_n}(r) R_{\alpha_p}(r) r^2 dr = \Omega_{\alpha}. \quad (5)$$

In the isospin-symmetry limit, the initial and final nuclear states, $|i\rangle$ and $|f\rangle$, are exact analog states and the radial overlaps

Ω_{α} are equal to unity. Then, Eq. (4) reduces to the model-independent value of the Fermi matrix element. Introducing charge-dependent interaction and a realistic single-particle basis, we can estimate deviations of the Fermi matrix element from its model-independent value.

It has been pointed out by Miller and Schwenk [15,16] that the exact isospin operator in (4) may involve terms where radial quantum number, n_{α} , for of a proton state α_p is different from that of a neutron state α_n . Here we notice that it is not possible to include those nondiagonal terms within the shell model because the nodal mixing requires very large model spaces. For this reason, we will stay within the same approximation as Towner and Hardy [2,4], considering only the diagonal terms.

Since the corrections considered here are small, we treat them within the perturbation theory. Let us define the correction to the one-body transition density due to the isospin-symmetry breaking as

$$\Delta_{\alpha} = \langle f | a_{\alpha_n}^{\dagger} a_{\alpha_p} | i \rangle^T - \langle f | a_{\alpha_n}^{\dagger} a_{\alpha_p} | i \rangle, \quad (6)$$

where the superscript T is used to denote the one-body transition densities calculated in the isospin-symmetry limit. Then, one can express the matrix element M_F in terms of Δ_{α} as

$$\begin{aligned} M_F &= \sum_{\alpha} (\langle f | a_{\alpha_n}^{\dagger} a_{\alpha_p} | i \rangle^T - \Delta_{\alpha}) \Omega_{\alpha} \\ &= \sum_{\alpha} (\langle f | a_{\alpha_n}^{\dagger} a_{\alpha_p} | i \rangle^T - \Delta_{\alpha}) [1 - (1 - \Omega_{\alpha})] \\ &= M_F^0 \left[1 - \frac{1}{M_F^0} \sum_{\alpha} \Delta_{\alpha} + \frac{1}{M_F^0} \sum_{\alpha} \Delta_{\alpha} (1 - \Omega_{\alpha}) \right. \\ &\quad \left. - \frac{1}{M_F^0} \sum_{\alpha} \langle f | a_{\alpha_n}^{\dagger} a_{\alpha_p} | i \rangle^T (1 - \Omega_{\alpha}) \right]. \end{aligned} \quad (7)$$

Since the isospin-symmetry-breaking effects are small, we can keep only the leading-order (linear) terms in small quantities and express M_F squared as

$$\begin{aligned} |M_F|^2 &= |M_F^0|^2 \left[1 - \frac{2}{M_F^0} \sum_{\alpha} \Delta_{\alpha} \right. \\ &\quad \left. - \frac{2}{M_F^0} \sum_{\alpha} \langle f | a_{\alpha_n}^{\dagger} a_{\alpha_p} | i \rangle^T (1 - \Omega_{\alpha}) + O(\zeta^2) \right], \end{aligned} \quad (8)$$

where ζ denotes $(1 - \Omega_{\alpha})$ or Δ_{α} . Comparing Eq. (8) with Eq. (2), we can identify the correction δ_C as a sum of two parts,

$$\delta_C = \delta_{IM} + \delta_{RO}, \quad (9)$$

called the *isospin-mixing* part,

$$\delta_{IM} = \frac{2}{M_F^0} \sum_{\alpha} \Delta_{\alpha}, \quad (10)$$

and the *radial-overlap* part,

$$\delta_{RO} = \frac{2}{M_F^0} \sum_{\alpha} \langle f | a_{\alpha_n}^{\dagger} a_{\alpha_p} | i \rangle^T (1 - \Omega_{\alpha}). \quad (11)$$

The initial and final state wave functions will be determined by diagonalization of a well-established shell-model effective Hamiltonian in a spherical (harmonic-oscillator) many-body basis. The isospin mixing part arises from the diagonalization of the shell-model Hamiltonian containing Coulomb and other charge-dependent terms. The parameters of such a Hamiltonian are usually adjusted to reproduce the splittings of the isobaric multiplets in a given model space. The estimate of the radial-overlap part of the correction, Ω_α , in Eq. (11) is calculated using realistic single-particle radial wave functions instead of the harmonic-oscillator wave functions. Thus, δ_{RO} accounts for the charge-dependent effects in the single-particle basis, which cannot be computed otherwise in a single-oscillator shell.

III. WOODS-SAXON POTENTIAL

A standard single-particle WS potential includes a spin-independent central term, a spin-orbit term, an isospin-dependent term, and a Coulomb term for protons:

$$V(r) = V_0 f(r, R_0, a_0) + V_s \left(\frac{r_s}{\hbar} \right)^2 \frac{1}{r} \frac{d}{dr} [f(r, R_s, a_s)] (\mathbf{l} \cdot \boldsymbol{\sigma}) + V_{\text{iso}}(r) + V_c(r), \quad (12)$$

where

$$f(r, R_i, a_i) = \frac{1}{1 + \exp\left(\frac{r - R_i}{a_i}\right)}, \quad (13)$$

with i denoting either 0 for the central term or s for the spin-orbit term. The radius is parametrized in a standard way as $R_i = r_i(A - 1)^{1/3}$, while the diffuseness parameters, a_i , are kept fixed. In general, the spin-orbit length parameter (r_s) is smaller than that of the volume term (r_0), because of the very short range of the two-body spin-orbit interaction [17]. The one-body Schrödinger equation is solved in relative coordinates for a particle of mass $\mu = m(A - 1)/A$, where m is the nucleon mass and A is the mass number of the composite nucleus. Among various terms of the WS potential, the last two terms are the most crucial for the radial-overlap correction.

Experimental data from both positive and negative energies suggested that an additional isospin-dependent term [18–20] was required. A common form of such a term [21,22], favoring a balanced configuration of neutrons and protons (symmetry term), reads

$$V_{\text{iso}}(r) = V_1 \frac{t_z T'_z}{A - 1} f(r, R_0, a_0), \quad (14)$$

where t_z is the isospin projection of the nucleon, with $t_z = 1/2$ for neutron and $-1/2$ for proton, and T'_z is the isospin projection of the core/target nucleus.

It was pointed out later by Lane [18,19] that the symmetry term (14) is an averaged version of a more fundamental formula which contains a dependence on the scalar product of the isospin operators of a nucleon (\mathbf{t}) and a core nucleus (\mathbf{T}') (see also discussion in Ref. [23]):

$$V_{\text{iso}}(r) = V_1 \frac{\langle \mathbf{t} \cdot \mathbf{T}' \rangle}{A - 1} f(r, R_0, a_0). \quad (15)$$

In principle, one could include other symmetry-preserving terms which involve the nucleon operators \mathbf{p} , \mathbf{r} , $\boldsymbol{\sigma}$, \mathbf{t} and the

TABLE I. Standard numerical values of the selected parametrizations.

	BM _m	SWV	Unit
r_0	1.26	1.26	fm
r_s	1.16	1.16	fm
$a_0 = a_s$	0.662	0.662	fm
V_0	-52.833	-652.0	MeV
V_1	-146.368	-133.065	MeV
λ	0.22	$0.198A^2/(A - 1)^2$	
λ_1	0.22	0	

core spin and isospin operators \mathbf{T}' and \mathbf{J}' . However, most of these terms were found to be small [20], except for the isospin-dependent spin-orbit term [24,25], important for study of neutron-rich nuclei:

$$V_{\text{iso}}^s(r) = V_1^s \frac{\langle \mathbf{t} \cdot \mathbf{T}' \rangle}{A - 1} \left(\frac{r_s}{\hbar} \right)^2 \frac{1}{r} \frac{d}{dr} [f(r, R_s, a_s)] (\mathbf{l} \cdot \boldsymbol{\sigma}). \quad (16)$$

Usually, the strength of the spin-orbit term is related to that of the volume term by $V_s = -\lambda V_0$, and similarly for the isospin-dependent part, $V_1^s = -\lambda_1 V_1$.

The repulsive long-range Coulomb potential is determined from the assumption of a uniformly charged sphere of radius R_c :

$$V_c(r) = (Z - 1)e^2 \times \begin{cases} \frac{1}{r} & \text{if } r > R_c, \\ \frac{1}{R_c} \left(\frac{3}{2} - \frac{r^2}{2R_c^2} \right) & \text{otherwise.} \end{cases} \quad (17)$$

For many applications, it is a good approximation because the influence of the surface diffuseness of the charge distribution on the strength of the Coulomb potential is not strong. In general, the radius R_c is defined in the same way as the central and spin-orbit radii: $R_c = r_c \times (A - 1)^{1/3}$. However, since the Coulomb term is of major importance for our study, we extract R_c from experimental data on charge radii, $\langle r^2 \rangle_{ch}$, via the expression [26]

$$R_c^2 = \frac{5}{3} \left[\langle r^2 \rangle_{ch} - \frac{3}{2} (a_p^2 - b^2/A) \right]. \quad (18)$$

In this equation, the last two terms correct for the internal structure of the proton and for the center-of-mass motion, with $a_p = 0.694$ fm [4] being the parameter of the Gaussian function describing the charge distribution of the proton and b being the harmonic-oscillator length parameter.

Among existing WS potential parametrizations (Refs. [17,23,27–30] and references therein), constructed with different objectives and relevant for different nuclear mass regions, we selected two (Table I). One is that of Bohr and Mottelson [17], modified as proposed in Ref. [31] and denoted as BM_m, while the other is that of Schwierz, Wiedenhöver, and Volya (SWV) [23]. They mainly differ by the isovector term: the BM_m parametrization adopts the symmetry term of the form of Eq. (14), whereas the other employs the isospin coupling as given in Eq. (15). For heavy nuclei with large neutron excess, the difference is small. For lighter nuclei around $N = Z$ line, which are of primary

interest for our study, the differences are important. Besides, the SWV parametrization defines radii with respect to the composite nucleus: $R_0 = r_0 A^{1/3}$ and $R_s = r_s A^{1/3}$.

IV. RADIAL OVERLAP CORRECTION IN THE CLOSURE APPROXIMATION

Although our final results are done within the parentage-expansion formalism, it is instructive to first consider the simplest approach which assumes that the ground state of the $(A - 1)$ nucleus is a unique parent (the formalism was outlined in Sec. II). Our purpose here is to study the parametrization dependence and to see better the role of the full parentage expansion presented in the next section.

We choose only sd -shell emitters, most of which are well described by the so-called universal sd interactions, USD and USDA/B [32,33]. They include ^{22}Mg , ^{26m}Al , ^{26}Si , ^{30}S , ^{34}Cl , ^{34}Ar , ^{38m}K , and ^{38}Ca . Six of these transitions are used to deduce the most precise $\mathcal{F}t$ value, while the decays of ^{26}Si and ^{30}S are expected to be measured with an improved precision in future radioactive-beam facilities. The shell-model calculations were performed in the full sd shell, using the NUSHELLX@MSU code [34].

To get the radial wave functions, we used two parameter sets of a WS potential summarized Table I. Note that these parameter sets have been determined by a global fit to various ground-state properties of nuclei around doubly-magic nuclei throughout the nuclear chart. The radial overlap correction is strongly dependent on the parametrization. In particular, it is very sensitive to the difference between proton and neutron single-particle states for an orbital with the same quantum numbers. One can also notice that the considered parametrizations do not account for the charge-symmetry-breaking effects which have been observed in nucleon-nucleon elastic scattering [35]. Furthermore, the charge symmetric isovector term (14) or (15) is related to the difference between neutron and proton numbers. For example, the radial overlap correction (almost) vanishes for $N = Z$ emitters. Obviously, this latter property does not agree with the HF case [14], because the isovector component of a self-consistent mean field is different from zero even in $N = Z$ nuclei due to the difference between proton and neutron densities.

To improve the accuracy of the WS potential, we keep the form of the potentials as described above and put the parameters under experimental constraints. In general, only the charge radii and the nucleon separation energies can be predicted by the WS model. In what follows, we readjust case by case the parameters r_0 and V_0 to reproduce the charge radii and the separation energies, respectively, while the other parameters are fixed at the standard values as given in Table I.

According to the Koopman's theorem, the energy of the highest occupied orbital is approximately equal to the nucleon separation energy with an opposite sign. Therefore, one usually fits the last occupied single-particle state and keeps the same potential to get all the other radial wave functions. For the present study, we readjusted V_0 for each valence orbital separately for protons and for neutrons. We believe that this method is more consistent with the shell model in which the valence single-particle states are partly occupied.

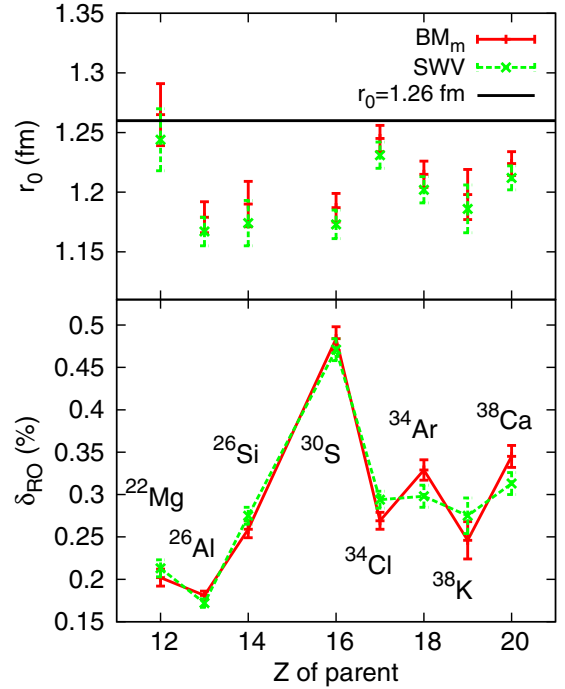


FIG. 2. Results with the adjusted parametrizations (BM_m and SWV) of a WS potential. The length parameter resulting from the fit of charge radii is plotted in the upper panel, the horizontal line indicates the standard value, $r_0 = 1.26$ fm. The radial-overlap correction, δ_{RO} , is plotted in the lower panel. These results are the averages of three values obtained with the USD, USDA, and USDB effective interactions. However, there is a great consensus about these interactions: the resulting uncertainties are negligible. The experimental data on ^{34}Ar and ^{38}K are taken from Ref. [36], while Ref. [4] is used for the others.

The charge radius is calculated via

$$\langle r^2 \rangle_{ch} = \int_0^\infty \rho_p(r) r^4 dr / \int_0^\infty \rho_p(r) r^2 dr + \frac{3}{2} (a_p^2 - b^2 / A). \quad (19)$$

with the proton density, $\rho_p(r)$, being

$$\rho_p(r) = \frac{1}{4\pi} \sum_{\alpha} |R_{\alpha p}(r)|^2 \times n_{\alpha p}. \quad (20)$$

The occupations $n_{\alpha p}$ are equal to $(2j + 1)$ for fully filled orbitals of an inert core, while for valence orbitals the occupation numbers are obtained from the shell-model diagonalization.

The values of the length parameter r_0 obtained from the fit of charge radii of the parent nuclei are plotted in the upper panel of Fig. 2, while the radial-overlap correction is shown in the lower panel. Notice that the two parametrizations produce very close results, confirming that the adjustment procedure puts severe constraints on the potential. We also remark that there is a pronounced odd-even staggering of δ_{RO} . Namely, for the parent nuclei with $(T_z = -1)$, we obtain a large overlap between proton and neutron radial wave functions, thus δ_{RO} increases. In cases of $T_z = 0$ emitters, the overlap is very close to unity, thus resulting in a very small correction value. This

effect is solely generated by the isovector terms, which also violate the isospin symmetry.

Two sources of uncertainties are considered: one is the error on the experimental data of charge radii and the other is the spread of results obtained with different shell-model effective interactions. We assume that the calculations with different interactions provide a set of independent values; we can thus apply statistics to describe this data set. Our adopted values are the normal averages (arithmetic means), while the spread of the individual values is considered a *statistical* uncertainty that follows a normal (or Gaussian) distribution. The uncertainties are dominated by the errors on the experimental charge radii and they only weakly depend on a particular effective interaction and a specific parametrization of the WS potential. For this reason, we consider this source of uncertainties to be *systematic*. To cover the small spread, the maximum value has to be chosen.

For each individual calculation, we compute the charge radii and the radial overlap correction for four different values of r_0 around 1.26 fm. Both quantities can be very well approximated by linear functions in the vicinity of 1.26 fm as

$$\begin{aligned}\sqrt{\langle r^2 \rangle_{ch}} &= a \times r_0 + b, \\ \delta_{RO} &= c \times r_0 + d,\end{aligned}\quad (21)$$

where a , b , c , and d are the regression coefficients.

Once these coefficients are determined, we can deduce the radial overlap correction and the length parameter that correspond to the experimental charge radii. To extract the systematic uncertainty on δ_{RO} we follow the error propagation rule,

$$\sigma_{\text{sys}} = \sqrt{(c \times \sigma_{r_0})^2 + (r_0 \times \sigma_c)^2 + (\sigma_d)^2}. \quad (22)$$

In this equation, σ_{r_0} is the systematic uncertainty on the length parameter, evaluated from the first line of Eq. (21), while σ_c and σ_d are the errors of the coefficients c and d , obtained from the fit. For all cases, the dispersion of the data points around the straight line is almost negligible, thus the errors σ_c and σ_d are generally not significant.

It is important to remark that σ_{sys} depends on the sensitivity to the length parameter [on a and c in Eq. (21)] which varies from nucleus to nucleus. This effect will be discussed in the next section.

The overall uncertainty is estimated as the sum in quadrature,

$$\sigma = \sqrt{\sigma_{\text{sys}}^2 + \sigma_{\text{stat}}^2}, \quad (23)$$

where σ_{stat} is the previously mentioned statistical uncertainty.

V. RADIAL OVERLAP CORRECTION WITH FULL PARENTAGE EXPANSION

A. Formalism

In the previous section, we took only the separation energies relative to the intermediate nucleus ground state. Now, we

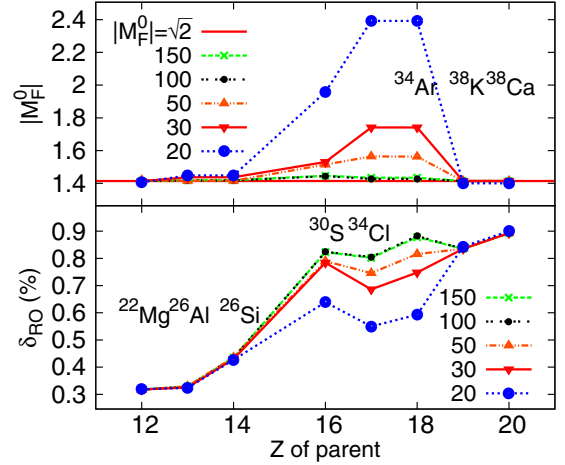


FIG. 3. Fermi matrix element $|M_F^0|$ and the radial overlap correction δ_{RO} for various numbers of intermediate states $N_\pi \in [20, 150]$.

extend our model as was done in Refs. [2,4,14] and expand δ_{RO} , inserting a complete sum over intermediate states $\sum_\pi |\pi\rangle \langle \pi|$ into the transition densities, between creation and annihilation operators. Hence, Eq. (11) becomes

$$\delta_{RO} = \frac{2}{M_F^0} \sum_{\alpha, \pi} \langle f | a_{\alpha_n}^\dagger | \pi \rangle^T \langle i | a_{\alpha_p}^\dagger | \pi \rangle^T (1 - \Omega_\alpha^\pi), \quad (24)$$

where the matrix elements $\langle f | a_{\alpha_n}^\dagger | \pi \rangle^T$ and $\langle i | a_{\alpha_p}^\dagger | \pi \rangle^T$ are related to the spectroscopic amplitudes [14] for neutron and proton pick-up, respectively. These quantities can be computed within the shell model using an appropriate isospin-invariant effective interaction. For the calculation of the overlap integrals, Ω_α^π , we take into account the excitation energies, E_π , in the intermediate nucleus while fitting the WS potential. Those excitation energies can be extracted from the experimental data, if available, or calculated theoretically.

In sd -shell nuclei, the basis dimensions for an intermediate nucleus can reach a few thousands. However, since spectroscopic amplitudes decrease on average with increasing excitation energy E_π , one can impose a robust truncation at a certain number of states, N_π . The variations of $|M_F^0|$ and δ_{RO} as a function of N_π are displayed in Fig. 3. From the top panel, it is seen that the Fermi matrix element does not converge quickly. For the transitions in the middle of the sd shell, with $N_\pi = 150$ for each spin and parity, the value of $|M_F^0|$ is still off its model-independent value. Fortunately, the correction δ_{RO} converges much faster than $|M_F^0|$, because of the factor $(1 - \Omega_\alpha^\pi)$ which decreases monotonically with increasing of E_π and tends to zero finally. For all sd -shell emitters, one can use $N_\pi = 100$ as a reasonable cutoff for the number of intermediate states.

B. Charge radius calculation

The parentage-expansion formalism can also be applied for the charge radius calculation. The square of the charge radius (relative to the inert core) is given by the expectation value of

the operator r_{sm}^2 in the ground state of a parent nucleus:¹

$$\begin{aligned} \langle r^2 \rangle_{sm} &= \langle \psi_i | r_{sm}^2 | \psi_i \rangle \\ &= \frac{1}{Z} \sum_{\alpha} \langle \alpha_p | r^2 | \alpha_p \rangle \langle i | a_{\alpha_p}^\dagger a_{\alpha_p} | i \rangle. \end{aligned} \quad (25)$$

Inserting the complete sum over intermediate states $\sum_{\pi} |\pi\rangle \langle \pi|$ into this equation, we convert the proton occupations, $\langle i | a_{\alpha_p}^\dagger a_{\alpha_p} | i \rangle$, into a sum of spectroscopic factors which can be obtained from the shell model. Thus, Eq. (25) takes the form

$$\langle r^2 \rangle_{sm} = \frac{1}{Z} \sum_{\alpha, \pi} \langle i | a_{\alpha_p}^\dagger | \pi \rangle^2 \langle \alpha_p | r^2 | \alpha_p \rangle^{\pi}. \quad (26)$$

The single-particle matrix element is given by

$$\langle \alpha_p | r^2 | \alpha_p \rangle^{\pi} = \int_0^{\infty} r^4 |R_{\alpha_p}^{\pi}(r)|^2 dr, \quad (27)$$

where π denotes that the radial wave functions depend on the intermediate states $|\pi\rangle$ because of the fit of separation energies. We have found that $\langle r^2 \rangle_{sm}$ as a function of N_{π} converges much faster than δ_{RO} . The value at $N_{\pi} = 50$ is sufficiently accurate.

Within the shell model exploited here, only a limited number of nucleons in a valence space outside an inert core are treated as active nucleons. In this spirit, we calculate the charge radii by two different methods. Following *method I*, we extract the contribution of core orbitals from the experimental charge radius, $\langle r^2 \rangle_{ch}^c$, of the closed-shell nucleus (i.e., ^{16}O for the *sd* shell) via

$$\begin{aligned} \langle r^2 \rangle_{ch} &= \langle r^2 \rangle_{sm} + \frac{3}{2} (a_p^2 - b^2/A) + \langle r^2 \rangle_{ch}^c \bar{Z} \\ &\quad + 3/4 (2n' + l' + 2) (b^2 - b_c^2) \bar{Z} \\ &\quad - 3/2 (a_p^2 - b_c^2/A_c) \bar{Z}, \end{aligned} \quad (28)$$

where $\bar{Z} = Z/Z_c$ is the ratio between the atomic numbers of parent and core nucleus. The third line of Eq. (28) accounts for the mass dependence of the potential. We obtained this term using harmonic oscillator wave functions (more details of the formalism can be found in Ref. [37]). The symbols n' and l' stand for the radial and orbital angular momentum quantum numbers of the highest filled level of the core, and b_c and A_c are the oscillator parameter and the mass number, respectively, of the closed-shell nucleus. The fourth line of Eq. (28) is the center-of-mass correction for the closed-shell nucleus, similar to that in Eq. (18). This method avoids the energy dependence of the nuclear mean field, which could be significant for deeply bound states, as suggested from the optical model [18–20] and also from HF calculations using Skyrme forces [38].

With *method II* we calculate the charge radii with WS eigenfunctions for all occupied states, including closed-shell orbits, following expressions (19) and (20). The proton occupancies

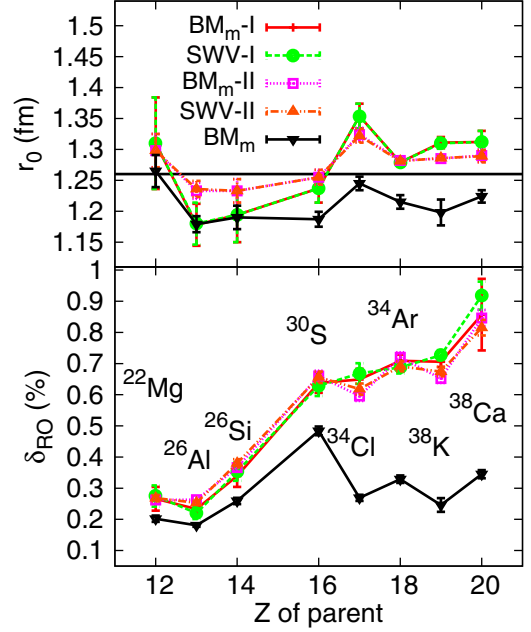


FIG. 4. The length parameter (upper panel) and radial overlap correction (lower panel) as obtained from method I (BM_m-I and SWV-I) and method II (BM_m-II and SWV-II). The horizontal line indicates the standard value of the length parameter, $r_0 = 1.26$ fm. The BM_m curve represents the values obtained in the closure approximation.

of core orbitals are taken as $(2j + 1)$. We notice that the energy dependence is not accounted for; however, this method is free from the mass-dependent correction which is necessary in the previous method.

We have explored the predictive power of these new approaches for charge radii. We found that, with V_0 as the only adjustable parameter, the predictive ability of our methods I and II is much better than that of the traditional approach, except for ^{34}Cl for which the value obtained from an isotope-shift estimation [4] is particularly large.

In the work of Towner and Hardy [2,4], the charge radii are computed via a simplified expression, Eq. (19), without intermediate states dependence. The resulting r_0 values are kept for the calculations of δ_{RO} in the full parentage-expansion formalism. In the latter step, the depth of the central term is independently readjusted to reproduce the separation energies with respect to multiple-intermediate states. We notice that, in principle, the two parameters could not be unambiguously determined in this way; instead the fit should be performed using the least-squares method, which ensures the optimization of the resulting radial wave functions.

Thanks to the generalization of the formalism for charge radii described above, we are able now to adjust both the potential depth V_0 and the length parameter r_0 in a self-consistent way. The final individual energy spectra and wave functions are thus capable of reproducing simultaneously the one-proton and one-neutron separation energies and the experimental charge radii of the parent nuclei. Our results with full parentage expansion are shown in Fig. 4 and tabulated in Table II. It is remarkable that the results obtained are very insensitive to the parametrization (SWV and BM_m). Moreover, the δ_{RO}

¹We diagonalize this operator in the initial 0^+ , $T = 1$ state. For most cases, it is the ground state of the parent nuclei, except for ^{26}Al and ^{38}K . For these two cases, such a state has an excitation energy of 228.3 and 130.4 keV, respectively.

TABLE II. Results of the calculations with full parentage expansion are tabulated with BM_m-I, SWV-I, BM_m-II, SWV-II, BM_m-IIG, and SWV-IIG (see Sec. V for details). Results obtained in our preliminary study, which did not include the multiple-intermediate states, are denoted by BM_m and SWV. These results correspond to those illustrated in Fig. 2. The values taken from Ref. [4] and from Ref. [2] (with partial updates from Ref. [1]) are reported with the labels TH2002 and TH2008 respectively.

Z	BM _m -I		SWV-I		BM _m -II		SWV-II		BM _m -IIG	
	r ₀ (fm)	δ _{RO} (%)	r ₀ (fm)	δ _{RO} (%)						
12	1.310(74)	0.266(38)	1.310(74)	0.275(34)	1.298(27)	0.262(12)	1.298(27)	0.268(10)	1.288(48)	0.253(17)
13	1.178(34)	0.233(18)	1.180(34)	0.220(19)	1.233(13)	0.263(7)	1.236(13)	0.253(7)	1.179(33)	0.245(9)
14	1.194(44)	0.339(35)	1.194(44)	0.353(29)	1.233(19)	0.366(11)	1.233(19)	0.380(13)	1.190(48)	0.345(21)
16	1.237(23)	0.638(32)	1.237(23)	0.629(33)	1.255(12)	0.660(17)	1.255(12)	0.656(18)	1.226(31)	0.637(21)
17	1.354(20)	0.649(34)	1.354(20)	0.668(33)	1.324(11)	0.596(16)	1.322(11)	0.618(18)	1.314(25)	0.536(25)
18	1.278(5)	0.708(20)	1.278(5)	0.686(20)	1.282(3)	0.720(16)	1.281(3)	0.691(16)	1.280(11)	0.636(11)
19	1.302(5)	0.680(11)	1.306(8)	0.714(21)	1.285(2)	0.652(14)	1.286(3)	0.674(15)	1.252(7)	0.538(8)
20	1.304(16)	0.889(42)	1.304(16)	0.869(46)	1.290(10)	0.846(26)	1.289(10)	0.815(25)	1.341(29)	0.761(39)
Z	SWV-IIG		TH2002		TH2008		BM _m		SWV	
	r ₀ (fm)	δ _{RO} (%)	r ₀ (fm)	δ _{RO} (%)						
12	1.263(48)	0.268(21)	1.281(26)	0.255(10)		0.370(20)	1.265(26)	0.202(10)	1.244(26)	0.213(10)
13	1.159(33)	0.219(13)	1.194(12)	0.230(10)		0.280(15)	1.179(13)	0.181(5)	1.167(12)	0.172(5)
14	1.168(46)	0.374(18)	1.206(18)	0.330(10)		0.405(25)	1.190(19)	0.259(10)	1.174(19)	0.275(10)
16	1.155(31)	0.616(25)	1.223(13)	0.740(20)		0.700(20)	1.187(12)	0.484(14)	1.173(12)	0.471(13)
17	1.214(26)	0.454(22)	1.303(11)	0.530(30)		0.550(45)	1.245(11)	0.269(10)	1.231(11)	0.294(10)
18	1.149(6)	0.587(18)	1.253(17)	0.610(40)		0.665(55)	1.215(11)	0.329(12)	1.202(11)	0.298(13)
19	1.162(9)	0.465(12)	1.245(21)	0.520(40)		0.565(50)	1.198(21)	0.246(22)	1.186(20)	0.275(21)
20	1.140(31)	0.670(36)	1.269(10)	0.710(50)		0.745(70)	1.224(10)	0.345(13)	1.212(10)	0.313(13)

correction depends little on the treatment of closed-shell orbits, and both methods produce consistent values throughout the *sd* shell. In general, the length parameters r_0 from method II are closer to a global-fit value of 1.26 fm [23]. In practice, method I is generally less appropriate for a charge radii fit because of its low sensitivity. Since the closed-shell contribution is taken from the experimental data, Eq. (28) puts little constraint on the valence space protons. Hence, the uncertainties on the BM_m-I and SWV-I results are much larger than those produced by method II.

Comparing the present results with those obtained in the closure approximation, Fig. 2, we remark that the introduction of multiple-intermediate states increases both the radial-overlap correction and the length parameter, especially for the transitions in the upper part of the *sd* shell.

C. Surface terms

Instead of varying the central part of the potential, one can include an extra surface-peaked term [39] and adjust its strength to reproduce the nucleon separation energies. Two terms have been considered in the literature [4], namely,

$$V_g(r) = \left(\frac{\hbar}{m_\pi c}\right)^2 \frac{V_g}{a_s r} \exp\left(\frac{r - R_s}{a_s}\right) [f(r, R_s, a_s)]^2 \quad (29)$$

and

$$V_h(r) = V_h a_0^2 \left[\frac{d}{dr} f(r, R_0, a_0) \right]^2, \quad (30)$$

where $(\hbar/m_\pi c) \approx 1.4$ fm is the pion Compton wavelength, while V_g and V_h are adjustable parameters.

We found that since $V_h(r)$ has a very weak effect on the single-particle spectra, the fit of separation energies results in very large values of V_h and generates a high peak on the WS potential at the nuclear surface. Besides, the inclusion of $V_h(r)$ leads to an unusual correlation between the charge radius and the length parameter: when r_0 increases, the calculated nuclear charge radius first increases and then decreases, following a kind of parabolic dependence. This property is in disagreement with the uniform-density liquid drop model [40], and moreover it deteriorates our optimization procedure. For these reasons, we do not use this term for our study of δ_{RO} .

In contrast, $V_g(r)$ has a much stronger effect on the single-particle spectra and does not lead to any particular problem in the fit. Before adding the surface term, we fix the depth of the central term, V_0 , in such a way that the calculated energy of the last occupied orbit matches the experimental separation energy relative to the ground state of the $(A - 1)$ nucleus. The energies of the remaining states are fitted by varying the strength of the surface term, while the parameter r_0 is consistently readjusted to get the experimental charge radii of the parent nuclei. The other parameters are kept fixed at the standard values. The obtained values of r_0 and δ_{RO} are shown in Fig. 5 (BM_m-IIG and SWV-IIG) in comparison to previously obtained results (BM_m-II and SWV-II).

First, we note that, except for a few cases, the addition of the $V_g(r)$ term produces larger charge radii, when r_0 is fixed. This is always the case for the SWV parametrization. As the radii are proportional to the length parameter, our fit with $V_g(r)$ results

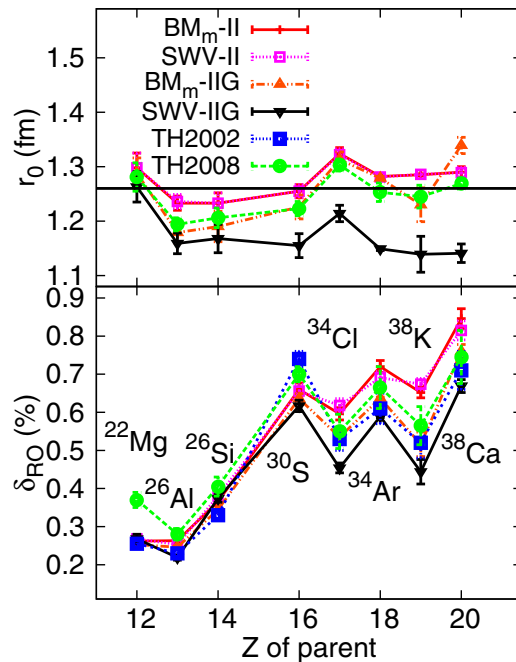


FIG. 5. The length parameter (upper panel) as obtained from method II and the corresponding radial overlap correction (lower panel). The horizontal line indicates the standard value of the length parameter, $r_0 = 1.26$ fm. BM_m -IIG and SWV-IIG refer to the calculations with BM_m and SWV parametrizations complemented by the surface term $V_g(r)$, while BM_m -II and SWV-II refer to the calculations without $V_g(r)$. For comparison we show the results of Towner and Hardy (TH2002 [4] and TH2008 [2]).

in smaller r_0 as seen from Fig. 5, except for ^{38}Ca (BM_m). In spite of smaller length parameters, the δ_{RO} values for the cases with masses between $A = 22$ and 30 are in fair agreement with those obtained in the calculations without $V_g(r)$. For the other transitions, the SWV-IIG values of δ_{RO} are about 25% lower than the BM_m -II or SWV-II values, whereas those obtained from the BM_m -IIG model drop only by about 15%. For heavier emitters, the inclusion of $V_g(r)$ leads to a clear dependence on the WS parametrization, even though the parameter V_0 also has been readjusted for the ground state. The uncertainties on these latter results are somewhat larger than those obtained from method II (see Table II). This means that the sensitivity to r_0 becomes lower [the coefficient c in Eq. (22) increases] when we include the $V_g(r)$ term.

D. Discussion

Figure 5 shows the comparison of the present results with the two results of Towner and Hardy (TH2002 [4] and TH2008 [2]). In Ref. [4], the shell-model calculations for nuclei between $A = 22$ and 34 have been performed in the sd shell; for $A = 38$, the $0f_{7/2}$ orbital has been added, with the $0d_{5/2}$ orbital being frozen. In 2008 [2], the authors introduced the core polarization in their calculation of δ_{RO} . Since then they evaluate the radial overlap correction with the inclusion of the orbitals outside the valence space, their method is based on shell-model calculations of the spectroscopic amplitudes, but limits the sums over single-particle orbitals to those for which

large spectroscopic factors have been observed in neutron pick-up reactions. Our work in this direction is in progress.

With the exception of ^{30}S , the BM_m -II or SWV-II values for δ_{RO} are on average 12% larger than those of TH2002. This augmentation could be understood as due to the increase of r_0 because our calculation takes into account all intermediate states for the charge radius. For $A = 38$, this effect may partly be due to the inclusion of $0f_{7/2}$ in the TH2002 calculation. A large value for ^{30}S reported in TH2002 may stem from different cutoffs for the sum over intermediate states. The values obtained in Ref. [2] (TH2008) with core-polarization effects are somewhat larger than their earlier result (TH2002), especially for ^{22}Mg . It can be seen from Fig. 5 that δ_{RO} from our SWV-IIG calculation follow closely the trend of TH2008, but they are about 16% smaller in magnitude. One may quickly guess that these two sets of δ_{RO} will produce a similar agreement with the CVC hypothesis, but with different $\mathcal{F}t$ values.

Note that the results of Towner and Hardy are obtained from their assessment of all multiple-parentage calculations made for each decay, including the calculation without additional terms and the calculation with the $V_h(r)$ and $V_g(r)$ terms. However, each of these calculations produced very similar values of δ_{RO} because they used the same set of the length parameter which is determined using a traditional method (see discussions in Ref. [4]).

We notice that the calculation with a surface-peak term could be very dependent on the fitting procedure. For example, if one fixes the depth of the volume term (V_0) to be the same for the proton and the neutron, then one adjusts the parameter V_g and r_0 to reproduce the relevant experimental observables, the conventional isovector terms present in the central part of the potential will not be affected or only weakly affected by this optimization procedure because of the difference between the form factor of the volume and the surface term. Consequently, the resulting δ_{RO} will show a stronger odd-even staggering, as we have seen in Sec. IV.

To conclude, we remind that the results of the shell-model plus WS wave functions predict δ_{RO} which are systematically larger than those from the shell model with HF wave functions [8,14]. The reason is the presence in the latter case of an additional self-consistent isovector potential which partially compensates for the difference between single-particle proton and neutron wells [14]. It may also be that addition of charge-symmetry breaking terms to a Skyrme force will result in larger values of the correction. The work in this direction is in progress and the results will be published elsewhere.

VI. CONSTANCY OF THE $\mathcal{F}t$ VALUES

With our results, we are now in a position to check the constancy of the $\mathcal{F}t$ values, the criterion to validate the CVC hypothesis. First, using our value for δ_{RO} and the input data for ft , δ_{NS} , δ'_R , and δ_{IM} from Ref. [1], we compute the individual $\mathcal{F}t$ values for each transition according to Eq. (1) and the corresponding uncertainty. Then, for six of these transitions we calculate the weighted average $\overline{\mathcal{F}t}$ (column 2 of Table III) for each method in comparison with the results of Towner and Hardy. The decays of ^{26}Si and ^{30}S are not included because of large experimental uncertainties on their ft values.

TABLE III. Reported in the left half (column 2 to 4) are the weighted averages, $\overline{\mathcal{F}t}$, and the corresponding χ^2/ν and CL values, while the right half (column 5 to 7) contains the values obtained from a similar procedure but without theoretical uncertainties on δ_{RO} . Labels for theoretical calculations: A = BM_m-I, B = SWV-I, C = BM_m-II, D = SWV-II, E = BM_m-IIG, F = SWV-IIG, G = TH2002, H = TH2008.

Model	With uncertainty of δ_{RO}			No uncertainty of δ_{RO}		
	$\overline{\mathcal{F}t}$	χ^2/ν	CL	$\overline{\mathcal{F}t}$	χ^2/ν	CL
A	3070.1(15)	5.09	0	3070.6(15)	6.97	0
B	3070.4(18)	6.45	0	3070.4(17)	8.94	0
C	3071.2(10)	2.84	1	3071.1(10)	3.08	0
D	3071.0(13)	3.93	0	3070.8(13)	4.35	0
E	3072.90(70)	1.06	38	3072.76(70)	1.25	28
F	3074.49(80)	0.46	81	3074.45(70)	0.49	78
G	3072.84(80)	1.92	9	3072.75(80)	2.02	7
H	3072.26(90)	0.57	72	3071.93(70)	0.82	54

For each average, we compute χ^2/ν , which measures the scatter of the individual $\mathcal{F}t$ values relative to the mean. Here $\nu = N - 1 = 5$ is the number of degrees of freedom. Then we use the scaling factor $s = \sqrt{\chi^2/\nu}$ to deduce the uncertainty on $\overline{\mathcal{F}t}$. The statistics procedure followed here is that recommended by the Particle Data Group [41].

In their latest survey [1], Hardy and Towner did not include any uncertainty on δ'_R , but treated the contribution of the $Z^2\alpha^3$ term in δ'_R as a source of systematic uncertainty, to be assigned to $\overline{\mathcal{F}t}$. In the present calculations, we adopt from that survey, adding into $\overline{\mathcal{F}t}$ a systematic uncertainty of ± 0.36 s, which corresponds to the contribution of the $Z^2\alpha^3$ term.²

From the obtained values of χ^2 , we proceed to calculate the confidence level (CL), defined as

$$p = \int_{\chi_0^2}^{\infty} P_\nu(\chi^2) d\chi^2, \quad (31)$$

where $P_\nu(\chi^2)$ is the χ^2 distribution function and χ_0^2 denotes the values computed with the null hypothesis (in our case, CVC is the null hypothesis). The calculated CL values for each model are given in Table III.

Method I produces the smallest values of $\overline{\mathcal{F}t}$, with the highest χ^2/ν . Under the assumption that CVC is valid, these results are statistically significant at $\text{CL} < 1\%$. We believe that this discrepancy reflects the inaccuracy of the δ_{RO} values generated by this method because of the sensitivity problem, as discussed in the previous section. Along these lines, the BM_m-I and SWV-I calculations must definitely be rejected. Concerning the results of method II, the agreement with CVC is somewhat better, but still significantly poorer than the two results of Towner and Hardy. In contrast, the calculations with $V_g(r)$ represent the best model for generating a set of

δ_{RO} corrections, satisfying the CVC hypothesis. The values resulting from the BM_m-IIG are of similar quality to those of TH2002, whereas the SWV-IIG calculation produces an even better CL and is comparable to that of TH2008.

In order to assess the constancy of the $\mathcal{F}t$ values from the eight sets of δ_{RO} on an equal footing, we perform a parallel analysis, by setting for all models the theoretical uncertainties on δ_{RO} to be equal to zero. The outcome is given in the right part of Table III, columns 5 to 7. It is seen that the omission of this source of uncertainties only slightly affects the weighted averages. The χ^2/ν values are systematically increased, thus resulting in a lower confidence level. Nevertheless, the conclusions of a comparative analysis of various methods remain unchanged.

However, it might be too early to draw any conclusion about the standard model because our samples are made up of only 6 out of the 14 best-known superallowed transitions. Our purpose is rather to provide, at least qualitatively, an alternative assessment for our theoretical models, and to compare with the previous calculations.

VII. CVC TEST FOR δ_{RO} CORRECTION

In this section, we carry out the confidence-level test proposed recently by Towner and Hardy [42], taking into account the experimental uncertainties, as well as uncertainties on δ_{RO} and the other theoretical correction terms. The test is based on the assumption that the CVC hypothesis is valid to at least $\pm 0.03\%$, which is the level of precision currently attained by the best ft -value measurements. This implies that a set of structure-dependent corrections should produce a statistically consistent set of $\mathcal{F}t$ values.

If we assume that the CVC hypothesis is satisfied ($\mathcal{F}t$ is constant), without regarding the CKM unitarity, we can convert those experimental ft values into experimental values for structure-dependent corrections and compare the results with each theoretical calculation in turn. Since the isospin mixing correction δ_{IM} is small compared to the radial overlap correction δ_{RO} and only one set of calculated δ_{NS} correction exists [43], pseudo-experimental values for δ_{RO} can thus be defined by

$$\delta_{RO}^{ex} = 1 + \delta_{NS} - \delta_{IM} - \frac{\mathcal{F}t}{ft(1 + \delta'_R)}. \quad (32)$$

To test a set of radial overlap correction for N superallowed transitions, we use the method of least squares with $\mathcal{F}t$ as the adjustable parameter, to optimize the agreement with the pseudo-experimental values:

$$\chi^2/\nu = \frac{1}{N-1} \sum_i^N \frac{[\delta_{RO}^{th}(i) - \delta_{RO}^{ex}(i)]^2}{\sigma_{th}(i)^2 + \sigma_{ex}(i)^2}, \quad (33)$$

where σ_{ex} and σ_{th} stand for the uncertainties on the experimental and calculated values of δ_{RO} respectively. The former is propagated from the right-hand side of Eq. (32), based on the data of ft , δ_{NS} , and δ'_R taken from Ref. [1].

Thus, the success of each theoretical calculation can be judged by the quality of the fit. The result for the renormalized $\mathcal{F}t$ is $\mathcal{F}t_R$, the optimized χ^2/ν is $[\chi^2/\nu]_{\min}$, and the

²To simplify, we take this value directly from Ref. [1]. Regarding their procedure, such uncertainty could depend on the sample size and on the calculated δ_{RO} values.

TABLE IV. Results similar to those given in Table III, except that $\mathcal{F}t$ is treated as an adjustable parameter. We added the subscript *min* to χ^2/ν to indicate the minimal or the optimized values. The corresponding $\mathcal{F}t$ values are referred to as renormalized values and denoted as $\mathcal{F}t_R$. The values listed in the left part result from the analysis that includes theoretical uncertainties on δ_{RO} , whereas those given in the right part are obtained without considering this uncertainty source.

Model	With uncertainty of δ_{RO}			No uncertainty of δ_{RO}		
	$\mathcal{F}t_R$	$[\chi^2/\nu]_{\min}$	CL	$\mathcal{F}t_R$	$[\chi^2/\nu]_{\min}$	CL
A	3067.43	0.14	98	3067.48	0.17	97
B	3066.81	0.10	99	3066.86	0.11	99
C	3069.09	0.17	97	3069.09	0.17	97
D	3068.45	0.19	97	3068.45	0.20	96
E	3071.82	0.25	94	3071.71	0.28	92
F	3074.18	0.26	93	3074.12	0.27	93
G	3071.22	0.41	84	3071.35	0.47	80
H	3071.13	0.22	95	3071.11	0.27	93

corresponding CL values are given in columns 2 to 4 of Table IV, while the values obtained without uncertainties on δ_{RO} are reported in columns 5 to 7. From both results, all eight sets of δ_{RO} (including those generated by method I) turn out to be very consistent with the CVC hypothesis with the optimized values of χ^2/ν ranging from 0.1 to 0.4 and the confidence level being greater than 80%. However, there is a significant spread among model calculations in the deduced $\mathcal{F}t_R$ values. It is seen that, with the exceptions of the BM_m -IIG and SWV-IIG models, the $\mathcal{F}t_R$ values are about 3 s lower than the weighted averages, $\overline{\mathcal{F}t}$, given in Table III.

From these results, we conclude that the statistical analysis of this section has very low comparative power. The result given in Table IV is not accurate enough to make a clear choice of one of the theoretical models. This indicates that the χ^2 test, Eq. (33), is not sensitive to small spreads between the correction sets. Obviously, although method I has been found to be inappropriate, the present analysis yields a good agreement of these correction values with the CVC hypothesis, comparable to the other calculations summarized in Table II. It is likely that a weak sensitivity of the χ^2 test based on Eq. (33) is due to the small number of transitions considered here, and the result should be reconsidered when more emitters are included. Too small χ^2/ν values may indicate too small values of uncertainties assigned to the corrections and should be revisited.

These results are preliminary. Firmer conclusions can be extracted when a whole series of emitters is examined in a similar way. We also remark that it would be interesting to reinvestigate $A = 38$ in a larger model space.

VIII. SUMMARY AND PERSPECTIVES

We have performed a detailed and critical study of the radial overlap correction, which is the major part of the isospin-symmetry-breaking correction to superallowed $0^+ \rightarrow 0^+$ β decay. Eight emitters in the sd shell have been reexamined,

using the USD, USDA, and USDB effective interactions, while the single-particle matrix elements of the transition operator are calculated with WS eigenfunctions.

We have investigated two WS potential parametrizations with different isovector terms, optimizing them in a two-parameter grid (r_0, V_0) to experimental nuclear charge radii and nucleon separation energies. As a new feature, we have introduced a parentage expansion to the nuclear charge radius, allowing us to perform a consistent adjustment of both parameters. All results have been thoroughly studied with respect to convergence as a function of the number of intermediate states. Two different approaches to nuclear charge radii with respect to the treatment of closed-shell orbitals and two different choices for adjusting the WS potential (variation of the central or surface term) led us to propose a set of six calculations of the correction for sd -shell nuclei. Two calculations have been found to be inappropriate because of their low sensitivity when treating the contribution of closed-shell orbits as a constant, taken from experimental radii of closed-shell nuclei. We found that the surface term, $V_h(r)$, is not compatible with our consistent adjustment, because of its very small effect on single-particle spectra.

For ^{22}Mg , ^{26}Al , and ^{26}Si , our values of δ_{RO} are close to those obtained by Towner and Hardy in 2002, when the same model space was exploited. All our models produced smaller values for ^{30}S . We suppose that this discrepancy is due to the difference in the cutoff for intermediate states. In the cases of ^{34}Cl , ^{34}Ar , ^{38}K , and ^{38}Ca , the correction is strongly dependent on the method of fitting the experimental data.

The calculated correction, δ_{RO} , combined with the radiative corrections (δ'_R and δ_{NS}) and experimental ft values from Ref. [1] leads to six new sets of corrected $\mathcal{F}t$ values. Four of these values are not concordant with the weighted averages for the six data points with a low confidence level. Nevertheless, the scatter is much reduced for the $\mathcal{F}t$ values resulting from the calculations with $V_g(r)$: the BM_m result has a CL of 38%, while the SWV result produces a CL of 81%.

With the assumption that CVC is valid, we performed the analysis considering the $\mathcal{F}t$ value as an adjustable parameter and minimizing the scatter between the calculated values of δ_{RO} and the pseudo-experimental values. This analysis shows that all sets of the correction generated by WS eigenfunctions agree well with the CVC hypothesis. Inclusion of other emitters may change this outcome.

It will be interesting to perform a similar study of lighter and heavier $0^+ \rightarrow 0^+$ emitters, as well as to enlarge the model space for nuclei near the cross shell using large-scale calculations. The aim is to explore the sensitivity of the results to details of the theoretical method and to robustly assign the corresponding uncertainties. The importance stems from the relevance to the most accurate tests of the standard model of electroweak interactions.

ACKNOWLEDGMENTS

We express our appreciation to B. Blank for his stimulating interest to this work, as well as to M. Bender for several interesting comments and suggestions for the theoretical part

and to T. Kurtukian-Nieto for her help with the statistical analysis. We also thank B. Blank and T. Kurtukian-Nieto for their careful reading of the manuscript and a number of useful comments. L. Xayavong would like to thank the University

of Bordeaux for support via a Ph.D. fellowship (2013-2016) provided in the framework of AAP “Recherche”. The work was supported as a part of the project “Théorie-ISB” by IN2P3/CNRS, France.

-
- [1] J. C. Hardy and I. S. Towner, *Phys. Rev. C* **91**, 025501 (2015).
[2] I. S. Towner and J. C. Hardy, *Phys. Rev. C* **77**, 025501 (2008).
[3] I. S. Towner and J. C. Hardy, *Phys. Rev. C* **91**, 015501 (2015).
[4] I. S. Towner and J. C. Hardy, *Phys. Rev. C* **66**, 035501 (2002).
[5] J. C. Hardy and I. S. Towner, *Phys. Rev. C* **79**, 055502 (2009).
[6] W. E. Ormand and B. A. Brown, *Phys. Rev. Lett.* **62**, 866 (1989).
[7] W. E. Ormand and B. A. Brown, *Phys. Rev. C* **52**, 2455 (1995).
[8] L. Xayavong, N. A. Smirnova, M. Bender, and K. Bennaceur, *Acta Phys. Pol. B. Suppl.* **10**, 285 (2017).
[9] W. Satuła, J. Dobaczewski, W. Nazarewicz, and M. Rafalski, *Phys. Rev. Lett.* **106**, 132502 (2011).
[10] H. Liang, N. V. Giai, and J. Meng, *Phys. Rev. C* **79**, 064316 (2009).
[11] N. Auerbach, *Phys. Rev. C* **79**, 035502 (2009).
[12] J. Damgaard, *Nucl. Phys. A* **130**, 233 (1969).
[13] E. Caurier, P. Navrátil, W. E. Ormand, and J. P. Vary, *Phys. Rev. C* **66**, 024314 (2002).
[14] W. E. Ormand and B. A. Brown, *Nucl. Phys. A* **440**, 274 (1985).
[15] G. A. Miller and A. Schwenk, *Phys. Rev. C* **78**, 035501 (2008).
[16] G. A. Miller and A. Schwenk, *Phys. Rev. C* **80**, 064319 (2009).
[17] A. Bohr and B. R. Mottelson, *Nuclear Structure Vol. I: Single-Particle Motion* (Benjamin, New York, 1969).
[18] A. M. Lane, *Phys. Rev. Lett.* **8**, 171 (1962).
[19] A. M. Lane, *Nucl. Phys.* **35**, 676 (1962).
[20] P. E. Hodgson, *Rep. Prog. Phys.* **34**, 765 (1971).
[21] G. R. Satchler, *Phys. Rev.* **109**, 429 (1958).
[22] A. E. S. Green and P. C. Sood, *Phys. Rev.* **111**, 1147 (1958).
[23] N. Schwierz, I. Wiedenhöver, and A. Volya, [arXiv:0709.3525](https://arxiv.org/abs/0709.3525).
[24] V. I. Isakov, K. I. Erokhina, H. Mach, M. Sanchez-Vega, and B. Fogelberg, *Eur. Phys. J. A* **14**, 29 (2002).
[25] V. I. Isakov, *Phys. At. Nucl.* **67**, 911 (2004).
[26] L. R. B. Elton, *Nuclear Sizes* (Oxford University Press, Oxford, 1961).
[27] Z. Łojewski and J. Dudek, *Acta Phys. Pol. B* **29**, 407 (1998).
[28] S. Cwiok, J. Dudek, W. Nazarewicz, J. Skalski, and T. Werner, *Comput. Phys. Commun.* **46**, 379 (1987).
[29] J. Dudek, Z. Szymański, T. Werner, A. Faessler, and C. Lima, *Phys. Rev. C* **26**, 1712 (1982).
[30] J. Dudek, A. Majhofer, J. Skalski, T. Werner, S. Cwiok, and W. Nazarewicz, *J. Phys. G* **5**, 1359 (1979).
[31] L. Xayavong, Ph.D. thesis, University of Bordeaux, 2016, <https://tel.archives-ouvertes.fr/tel-01674248>.
[32] B. H. Wildenthal, *Prog. Part. Nucl. Phys.* **11**, 5 (1984).
[33] B. A. Brown and W. A. Richter, *Phys. Rev. C* **74**, 034315 (2006).
[34] B. A. Brown and W. D. M. Rae, *Nucl. Data Sheets* **120**, 115 (2014).
[35] H. Fearing, *Nucl. Phys. A* **353**, 17 (1981).
[36] I. Angeli and K. Marinova, *At. Data Nucl. Data Tables* **99**, 69 (2013).
[37] M. W. Kirson, *Nucl. Phys. A* **781**, 350 (2007).
[38] C. B. Dover and N. V. Giai, *Nucl. Phys. A* **190**, 373 (1972).
[39] W. Pinkston and G. Satchler, *Nucl. Phys.* **72**, 641 (1965).
[40] G. Gamow, *Proc. R. Soc. London A* **126**, 632 (1930).
[41] C. Amsler *et al.* (Particle Data Group), *Phys. Lett. B* **667**, 1 (2010).
[42] I. S. Towner and J. C. Hardy, *Phys. Rev. C* **82**, 065501 (2010).
[43] I. S. Towner and J. C. Hardy, *Lett. B* **333**, 13 (1985).